Fuel 196 (2017) 298–305

Contents lists available at ScienceDirect

Fuel

journal homepage: www.elsevier.com/locate/fuel

Full Length Article

Process modeling of hydrodeoxygenation to produce renewable jet fuel and other hydrocarbon fuels

Pei Lin Chu [a], Caroline Vanderghem [a], Heather L. MacLean [a,b,c], Bradley A. Saville [a,*]

[a] Department of Chemical Engineering and Applied Chemistry, University of Toronto, Toronto, Ontario M5S 3E5, Canada
[b] Department of Civil Engineering, University of Toronto, Toronto, Ontario M5S 1A4, Canada
[c] School of Public Policy and Governance, University of Toronto, Toronto, Ontario M5S 3K9, Canada

HIGHLIGHTS

- Composition of feedstock oils affects product distribution and hydrogen demand.
- Feedstock affects thermal and electrical energy requirements.
- Oil content of the oilseed is a key parameter.
- Strategic heat integration reduces thermal energy demand.

ARTICLE INFO

Article history:
Received 7 August 2016
Received in revised form 27 January 2017
Accepted 28 January 2017
Available online 14 February 2017

Keywords:
Synthetic paraffinic kerosene (SPK)
Hydroprocessed renewable jet (HRJ)
Biojet fuel
Camelina
Carinata
Used cooking oil

ABSTRACT

The focus of this work is to model the hydrodeoxygenation process to produce renewable jet fuel and co-products from low-input oilseeds, specifically camelina, carinata (non-edible oil) and used cooking oil (UCO), taking into account the fatty acid compositions by incorporating the stoichiometric hydrodeoxygenation reactions. This methodology provides insight into the effect of feedstock composition and hydrodeoxygenation reactions upon product yields, product distribution, hydrogen consumption and process utilities. The resulting product slates, hydrogen gas and utility demands are specific to each of the camelina, carinata and UCO feedstocks.

The yield of kerosene-range alkanes ranged from 53 to 54% of the incoming oil, with 13–14% diesel range alkanes, 13–15% naphtha, and 7–9% liquefied petroleum gas, depending upon the fatty acid composition. The hydrogen consumption rate ranged from 26 to 30 kg per tonne of incoming oil, depending upon the degree of bond unsaturation. Thermal energy demand is 2.8 GJ/tonne oil when processing used cooking oil, versus 5.2 and 5.7 GJ/tonne of oil for carinata and camelina, respectively, owing to the additional energy required for oil extraction. Electricity demand was 73 kWh/tonne oil for UCO, versus 170 and 227 kWh/tonne oil for carinata and camelina.

1. Introduction

The aviation industry relies on petroleum-based fuels, but potential adverse environmental impacts from these fuels have been identified. The combustion of fossil fuels is of particular concern due to the impact of greenhouse gas (GHG) emissions on climate change. Development of low GHG intensity fuels is an emerging frontier to address growing climate change concerns in the aviation industry.

The International Air Transport Association (IATA) has responded by creating an emission reduction roadmap, which aims to lessen the environmental impact of air travel by improving fuel efficiency by 1.5% annually until 2020; achieve carbon neutral growth beyond 2020; and halve overall aviation emissions from 2005 levels by 2050 [1–3]. The EU Emission Trading Scheme (ETS) based on a "cap and trade" system also aims to reduce emissions [4]. As of 2012, airlines operating or providing services within the European Economic Area (EEA) are subject to the ETS, although the aviation industry was temporarily exempted from the ETS while the EU negotiates an agreement with the International Civil Aviation Organization (ICAO). The ETS is currently only applicable to flights within the EEA; a global market-based mechanism is being developed by ICAO to cover international aviation emissions, to be implemented by 2020 [5].

* Corresponding author.
E-mail address: bradley.saville@utoronto.ca (B.A. Saville).

http://dx.doi.org/10.1016/j.fuel.2017.01.097
0016-2361/

Biojet produced from the hydrodeoxygenation (HDO) process is currently one of the biofuels used in demonstration and commercial flights. It is also a technology that has been commercialized to produce renewable diesel. Due to its technological maturity, it is expected that this pathway will play a major role in producing low carbon intensity jet fuels. The HDO process to produce hydroprocessed renewable jet (HRJ) from triacylglycerides (TAG) includes hydrogenation, deoxygenation, isomerization and hydrocracking stages. Hydrogenation is the first reaction, saturating all TAG bonds. Deoxygenation follows hydrogenation, and consists of three parallel reactions, including decarboxylation, decarbonylation and hydrodeoxygenation, as illustrated in Fig. 1 (adapted from Veriansyah et al. [6]). The alkanes produced are referred to as synthetic paraffinic kerosene (SPK) or HRJ, and are commonly known as hydroprocessed esters and fatty acids (HEFA) SPK. HDO fuel products are molecularly similar to their petroleum counterparts, with the notable difference being a lack of aromatic content. The TAG can be from diverse virgin and used oil feedstocks. Based on the fatty acid composition of the feedstock, the product yields, product distribution, hydrogen consumption and process utilities of the HDO process might vary, perhaps considerably. This issue, however, has not previously been investigated, and a key objective of this work is to rigorously evaluate the impact of fatty acid composition upon these key operating parameters.

UOP is a leading technology provider for the HDO process and has partnered with several biofuel producers, such as Altair and Ensyn, to convert vegetable oils and pyrolysis oil into liquid fuels, respectively. UOP has also developed their Green Jet Fuel™ Process (Fig. 2) using proprietary multifunctional catalysts [7] to target the production of HRJ. The catalysts selectively hydrocrack the deoxygenated fatty acids, to maximize production of jet fuel range alkanes while reducing the co-production of lower value lighter hydrocarbons. Since the process is patented, the specific reaction conditions, including its product slate, are not publicly available. The UOP process has produced fuels for most of the biojet test flights using vegetable oils.

Most studies assume that the production of biojet from lipids is independent of the feedstock oil and fatty acid profiles, and that the conversion of fatty acids produces only alkanes, carbon dioxide and water [9–13]. These assumptions do not account for the different degree of saturation of fatty acids, which would affect the H_2 needed for the hydrogenation reaction that converts TAG into fatty acids and propane. Stratton's LCA work to screen biojet production pathways examined the cracking reaction based solely on *n*-octadecane, a representative C18 molecule, which may not accurately represent the co-production of naphtha or other shorter alkanes when a diverse alkane pool is present [9]. Subsequent publications using data from Stratton [9] have incorporated this simplified view of the conversion process. While helpful for an initial evaluation, these simplifying assumptions do not reflect actual conversion reactions. This was later addressed by Pearlson [14,15]; using product yields from the literature for diesel products from soybean oil and jet fuel yields from jatropha oil, he calculated product yields including co-products such as propane, LPG and naphtha. However, Pearlson [14] has generalized the yield and conversion based upon soybean oil. Han et al. [13] pointed out the need to tailor the hydrogen (H_2) requirements based on the oil feedstock composition, but assumed the complete conversion of diesel into biojet [13], which is unlikely based upon typical cracking reactions and process technology.

The aim of this work is to model the HDO process from *Camelina sativa* (camelina), *Brassica carinata* (carinata), and used cooking oil (UCO), quantifying the H_2 demand, energy, electricity requirements and product slate from each set of triglycerides. Due to the scarcity of technology specific data such as for the UOP process, the modeling work is based on published studies describing the HDO conversion of fatty acids into paraffins. The methodology developed in this study will provide insight into the impact of feedstock composition upon product yield and hydrogen gas consumption. These parameters are crucial when modeling the HDO process, to quantify the total thermal energy and electricity demands and corresponding GHG emissions for the jet fuel product, when coupled with information on the thermal energy source and electricity grid. Results of the study also serve as a benchmark for comparison against literature data that used simpler modeling approaches, with soy oil and jatropha oil as feedstocks.

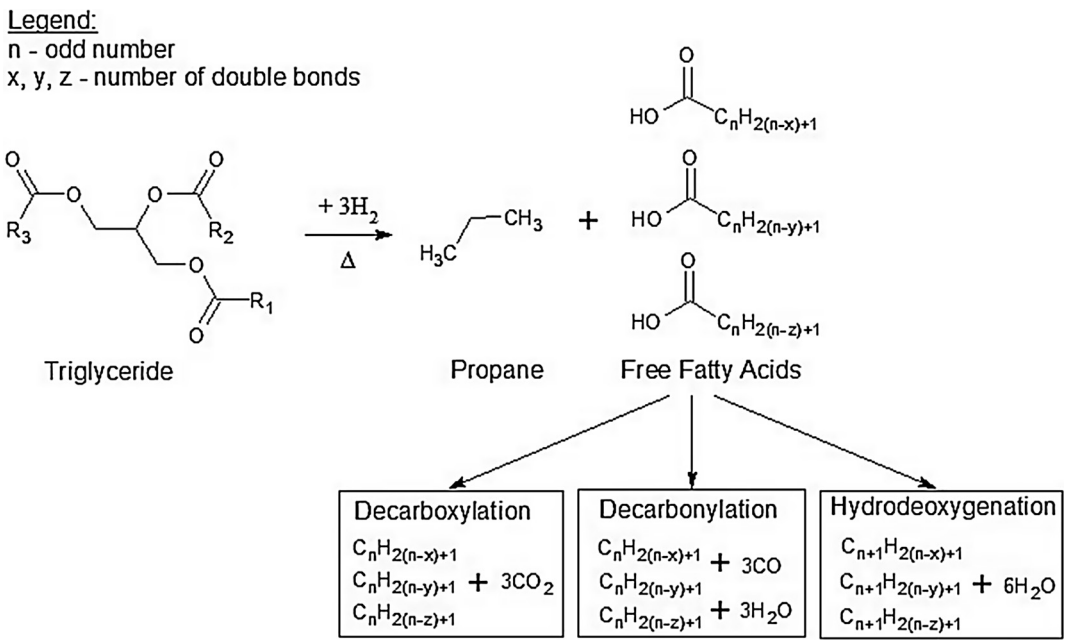

Fig. 1. The chemistry of hydrocracking of a TAG molecule that produces carboxylic acids and propane. The carboxylic acids subsequently undergo oxygen removal reactions. Adapted from Veriansyah et al. [6].

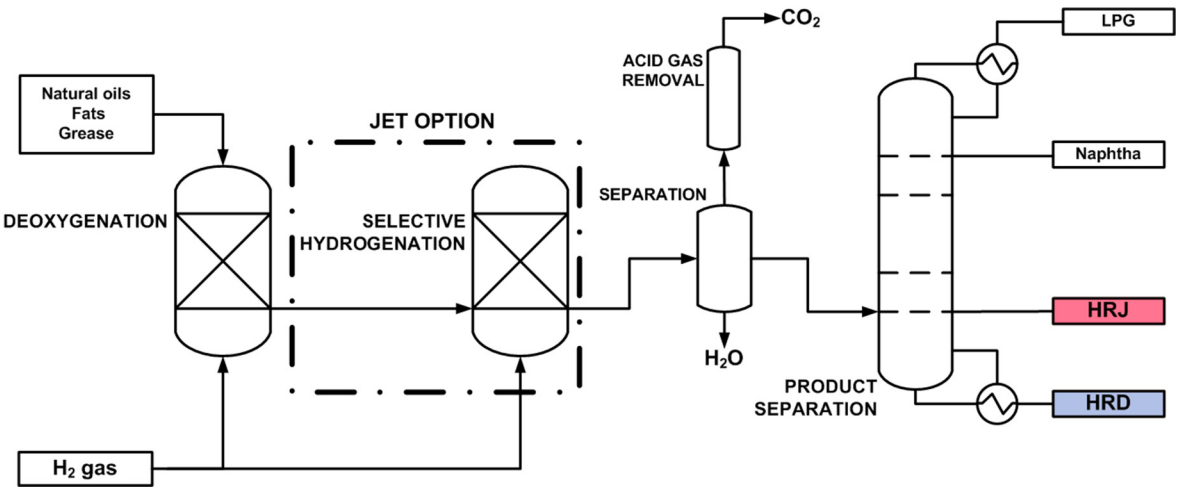

Fig. 2. Process schematic of the UOP Green Jet Fuel™ process to produce HRD from natural oils, fats and grease with the selective hydrogenation process options to maximize HRJ production. Adapted from UOP [8]. Note: HRJ = hydroprocessed renewable jet, HRD = hydroprocessed renewable diesel.

2. Process simulation scope and methodology

Biojet production using the HDO process is comprised of four different processes, including feedstock production, oil extraction, fatty acid conversion to renewable alkanes and product recovery, as described below. Oil extraction is omitted from the model when processing UCO. The processes to produce and recover renewable alkanes were modeled using the Aspen Plus simulation software [16]. The reactions and conversions for each fatty acid were modeled in Microsoft Excel, and the aggregate conversion, product distribution and hydrogen demand were calculated based upon the fatty acid composition of the oil from each type of feedstock.

2.1. Feedstock production

Camelina and carinata are seasonal crops with growing seasons of 80–120 days. These crops produce oilseeds with high oil content, and can grow on semi-arid land that is normally unsuitable for conventional crop production [17]. Spring and winter varieties are currently under development for use on fallow lands, with the potential for double cropping [18]. These crops also require less agricultural inputs than conventional crops, which lower production costs and GHG emissions, while still achieving high productivity [19].

Used Cooking Oil (UCO) was also selected as it is a near-term feedstock for biojet production. UCO is produced in the food industry, especially in major urban centers, is a traded commodity, and can be used as a feedstock for the HDO process.

2.2. Solvent extraction

Process details and specifications for oil extraction have been described in the literature, including the industrial solvent extraction process for edible oils processing [20] and oil extraction in the canola industry [21]. The processing and handling of camelina and carinata are assumed to be the same as for canola, due to the similarity in seed dimensions and oil content. Oilseed characteristics for camelina and carinata are outlined in Table 1. Oil extraction operations include seed cleaning, crushing, cooking with direct steam injection, mechanical extrusion, flaking, countercurrent solvent extraction, meal toasting and drying, and solvent stripping (Fig. 3). UCO does not require an extraction step.

When the oilseeds are received, they are initially screened to remove field dirt and metals. To prevent seed shatter, the seeds are heated using injected live steam before crushing in roller mills. The cooked seeds are then extruded mechanically at high temperature and pressure to remove most of the oil. The subsequent chemical process saturates the seeds with a solvent, usually hexane, creating a mixture that is recovered from the seeds by solvent stripping to separate the oil product and recover the solvent for reuse.

Table 1
Oilseed characteristics used in estimating the solvent extraction mass balance, Rispoli [22].

	Camelina, wt.%	Carinata, wt.%
Moisture	9.0	9.0
Fibre	13.5	19.0
Protein	42.5	28.0
Oil	35.0	44.0

The oil extraction process is the most energy intensive step during the oil extraction stage. Although mechanical extraction processes require less energy, the mechanical + chemical method was selected for its higher oil recovery, which is crucial when the cost of feedstock dominates the process economics.

2.3. Oil conversion

The conversion of oil into fuels occurs in a pressurized hydrotreating reactor at high temperatures. The extracted oil is fed with compressed hydrogen into the reactor, which contains a nickel–molybdenum (NiMo) or similar catalyst. The selectivity of cracking is difficult to control, influenced by the catalysts used and the reaction conditions [23,24]. A natural gas boiler provides the heat needed to maintain the reaction temperature. Light hydrocarbons generated as co-products of the process may also be used for this purpose, or fed to a reforming unit to produce the hydrogen necessary for the process. The operating parameters used during the oil conversion process modeled in Aspen Plus, based upon a NiMo catalyst, are outlined in Table 2.

The high pressure and temperature vapor exiting the reactor is fed to a turbine to generate electricity that provides power to the process. The conversion process, including electricity generation, is illustrated via the block flow diagram in Fig. 4.

Oil conversion in the HDO process revolves around the decarboxylation, decarbonylation and hydrodeoxygenation reactions outlined in Table 3. The decarboxylation reaction removes oxygen

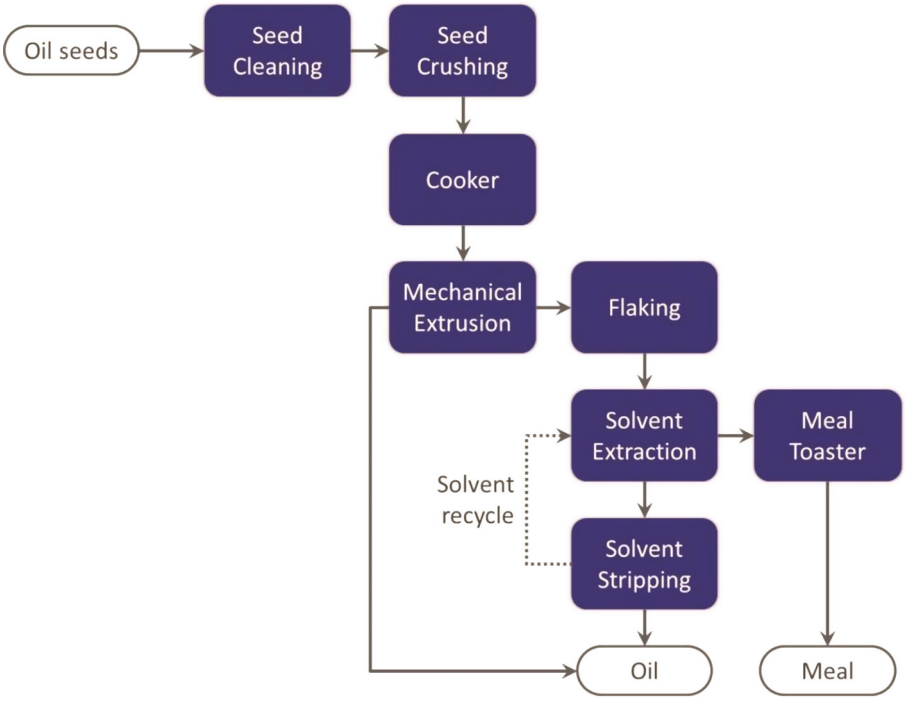

Fig. 3. Block flow diagram of conventional solvent extraction process.

Table 2
Input data and assumptions for the HDO process model [6,25].

Process parameter	Value
Reaction temperature	400 °C
Reaction pressure	92 bar
Residence time	2 h
Catalyst type	NiMo
Conversion, X (batch operation)	0.9994
Extent of decarboxylation, ε1	0.68
Extent of decarbonylation, ε2	0.03
Extent of hydrodeoxygenation, ε3	0.29
Aspen reactor model	RStoic
Property method	NRTL & Peng-Robinson

through C—C bond scission to form CO_2 in the absence of H_2 gas (Eq. (1)), while the decarbonylation reaction uses H_2 gas through C—O bond scission to remove oxygen, generating CO and water (Eq. (2)). Both reactions produce alkanes with one less carbon than the original fatty acid. On the other hand, the hydrodeoxygenation reaction uses H_2 to remove oxygen and produce water, thereby preserving the carbon content of the original fatty acid (Eq. (3)). The hydrogen requirement for the HDO process is dependent on the selectivity between the oxygen removal reactions. The reaction conditions and selected catalyst can impact the extent and selectivity of the three competing reactions, which can be optimized for biojet production. The oxygen removal reactions during the HDO process occur in the liquid phase to produce gaseous reaction products. These gases are suspected to react with H_2 gas, causing methanation (Eq. (4)) and water-gas-shift (Eq. (5)) reactions to produce CO_2, methane and water. This leads to the production of lighter products and increased the demand for H_2 gas.

The reactions and conversions were modeled in Microsoft Excel based upon each fatty acid in the oilseed (Table 4). This approach overcomes the limited number of fatty acid components in the Aspen Plus databank. A mass balance for the oil conversion process was generated using the stoichiometric reactions that would occur during the process. These reactions and the mass balance were used to calculate the amount of hydrogen gas required and the amount of CO_2, CO and water produced. As shown in Table 4, there can be substantial differences in the content of saturated, monounsaturated and polyunsaturated fatty acids, which should affect hydrogen demand. Camelina, carinata and UCO oils have high degrees of monounsaturated and polyunsaturated fatty acids.

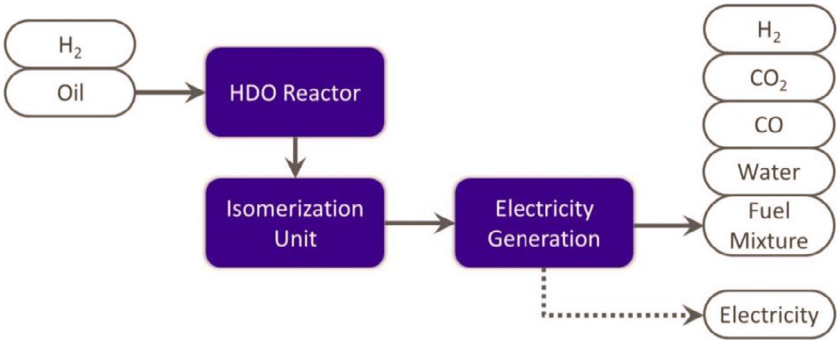

Fig. 4. Block flow diagram of the oil conversion process.

Table 3
Stoichiometric reactions involved in the HDO process [26].

	Stoichiometric reaction	ΔH_{573} (kJ/mol)
Eq. (1) Decarboxylation	$C_nH_{2n}O_2 \rightarrow C_{n-1}H_{2n} + CO_2$	9.2
Eq. (2) Decarbonylation	$C_nH_{2n}O_2 + H_2 \rightarrow C_{n-1}H_{2n} + CO + H_2O$	179.1
Eq. (3) Hydrodeoxygenation	$C_nH_{2n}O_2 + 3H_2 \rightarrow C_nH_{2n+2} + 2H_2O$	−115.0
Eq. (4) Methanation	$CO_2 + 4H_2 \leftrightarrow CH_4 + 2H_2O$	−177.2
	$CO + 3H_2 \leftrightarrow CH_4 + H_2O$	−216.4
Eq. (5) Water gas shift	$CO + 4H_2 \leftrightarrow H_2 + CO_2$	−39.2

Camelina oil is mainly composed of polyunsaturated fatty acid (54.3 wt.%), in which the main fatty acid is linolenic acid (C18:3; 32.6 wt.%). Carinata oil is mainly oleic acid (C18:1; 43.2 wt.%) followed by linoleic acid (C18:2; 36.0 wt.%). The majority of fatty acids in UCO are linoleic acid (C18:2; 43.0 wt.%) followed by oleic acid (C18:1; 36.0 wt.%). Fatty acid compositions of soybean, palm, rapeseed and jatropha oils are included in the table for comparison. Soybean oil has a high degree of polyunsaturated fatty acids (C18:2; 53.0 wt.% and monounsaturated fatty acids (C18:1; 22.0 wt.%). Rapeseed oil is comprised of 70 wt.% monounsaturated fatty acids (C18:1; C20:1 and C22:1). Jatropha oil has a higholeic acid (C18:1; 45.0 wt.%) and linoleic acid (C18:2; 34.0 wt.%) content. In contrast, palm oil is highly saturated (C16:0; 40.8 wt.%).

The product distribution was determined based upon the percentage of oil processed through each of the decarboxylation, decarbonylation and hydrodeoxygenation reactions (Table 3), while accounting for likely/possible cracking at the double bond sites in each fatty acid (which leads to different products dictated by the fatty acid composition). A theoretical minimum amount of H_2 gas required for the HRJ facility was calculated, which formed the basis for the subsequent modeling in Aspen Plus [16]. This was replicated for all fatty acids to obtain the overall mass balance, H_2 gas requirement and the product slate that are specific for each oil fatty acid profile. Using the inputs and yields from the Excel model for camelina, carinata and UCO, the HDO process was simulated for each feedstock in Aspen Plus to obtain overall mass and energy balances.

2.4. Product recovery

The product stream leaving the turbine is a mixture of fuel products that requires separation, much like a conventional oil refinery. The products are separated using multiple distillation columns to produce fuels that meet the specifications for their intended use.

The first separation stage is a "gas-liquid separation" that removes non-condensable gases, such as carbon dioxide (CO_2), carbon monoxide (CO), and excess hydrogen from the reactor. These gases leave the top of the separation column and are combusted by a flare to ensure no combustible gases are emitted to the atmosphere. The liquid products are first processed in a prefractionator column that separates the lighter (C1-C6) and heavier (>C7) products. Light products are sent to the stabilizer column to isolate LPG (C1-C4) products from light naphtha (>C5). The heavy products are processed in a crude distillation unit to separate the various cuts into heavy naphtha (C6-C9), kerosene (C10-C15) and diesel (>C15). The fuel products are stored onsite.

Process heat for the distillation columns is supplied by steam produced in a natural gas boiler, while electricity is provided from the on-site turbine and from the local power grid. Cooling is supplied using a standard water cooling tower system. The energy required during product recovery (due to the number of distillation columns for separation) is a major contributor to overall process energy demand. The specifications for the separation columns modeled are summarized in Table 5, and illustrated as a block flow diagram in Fig. 5.

3. Results and discussion

3.1. Product slates

Modeling of the conversion reactions in Microsoft Excel produced a mass balance as well as the expected product slate for each feedstock based upon its fatty acid profile. Mass balance results from this study for the three feedstocks are presented in Table 6. Results from the literature (Pearlson [14] and Han et al. [13]) are included in the table for comparison. The HDO process is governed by the reactions outlined in Table 3 and the production of light products is inevitable. Based on the molecular composition for each of the feedstocks examined, there is a minimum amount of hydrogen gas that is required to cleave the glycerol backbone, which is subsequently converted into propane, while producing free fatty acids. The free fatty acids can then undergo decarboxylation, decarbonylation or hydrodeoxygenation reactions. The selectivity of the fatty acids to undergo either of these deoxygenation reactions is dictated by the catalysts used and process conditions. Considering the chain length of the fatty acids, for instance C18:0, cracking of the fatty acid will generate a light fraction (e.g., C1-C6) and a heavy fraction (e.g., C12-C17). Even though the lighter fractions are not desired, in order to generate valuable heavier fractions such as kerosene and diesel, it is necessary to

Table 4
Fatty acid profiles of camelina, carinata, and used cooking oil (UCO), with comparison to other oils.

Fatty acid (wt.%)	Camelina[a]	Carinata[b]	UCO[c]	Soybean[d]	Palm[d]	Rapeseed[d]	Jatropha[d]
<C14	0	0	0	0	5.2	0	0
C14:0	0.1	0	0	0	1.3	0	0
C16:0	6.8	5.4	13.0	11.0	40.8	3.0	13.0
C18:0	2.7	0.2	3.8	4.0	3.7	1.0	8.0
C20:0	1.5	0.0	0	0	0	0	0
C22:0	0.2	0.0	0	0	0	0	0
C18:1	18.6	43.2	36.0	22.0	37.2	17.0	45.0
C20:1	12.4	0	0	0	0	11.0	0
C22:1	2.3	0	0	0	0	45.0	0
C18:2	19.6	36.0	43.0	53.0	10.1	14.0	34.0
C18:3	32.6	15.2	3.6	8.0	0	9.0	0
C20:2	1.3	0	0	0	0	0	0
C20:3	0.8	0	0	0	0	0	0

[a] From [27].
[b] From [28].
[c] From [29].
[d] From [13].

Table 5
Input data for modeling of hydrocarbon product separation.

Unit	Aspen block	Number of stages	Column pressure
Prefractionator	PetroFrac	15	2.5 bar
Stabilizer	RadFrac	20	15.5 bar
Crude Distillation Unit (CDU)	PetroFrac	21	1 bar

crack the longer chains. Some would argue that cracking is not necessary for C18:0, but in the HDO reactor, cracking can occur in the midst of decarboxylation, decarbonylation and hydrodeoxygenation reactions, and it is difficult to control the degree of cracking. Nonetheless, cracking can be minimized by lowering the reaction temperature, altering the reaction pressure and the use of selective catalysts. Theoretically, it is not possible to avoid producing lighter fractions or processing the heavier fractions. If the heavy fractions are further processed, more light hydrocarbons would be observed in product distribution. In a process that targets the production of HRJ, where the diesel fraction is further cracked into kerosene-range hydrocarbons, additional light hydrocarbons are inevitably produced. Historically, diesel has a slighter higher market value than kerosene, and therefore, producers have little to no motivation to invest more capital and convert a higher value product, i.e., diesel, into a lower value product. Therefore, it is not realistic for a refinery to continuously crack diesel into lighter fractions to maximize kerosene output.

Although the differences in fatty acid composition have yielded different mass balance results, these differences for an individual oilseed/oil are small relative to the compositional differences between different oilseeds, and thus, the observed trends illustrating differences in the product slate and hydrogen requirements between feedstocks should remain consistent. By comparison, the product slate and mass balances in Pearlson's work [14] are independent of feedstock composition. It should be noted that kerosene yields in Han et al. [13] are higher compared to our work and Pearlson's work, due to Han's assumption of complete conversion of diesel into kerosene. CO_2, CO and water values were not reported by Han et al. [13].

3.2. Process energy demand

The heating and cooling requirements for the HDO process were calculated using Aspen Plus, and are presented in Table 7. Heat integration using pinch analysis was performed in order to model a realistic production facility. The highest energy recovery was obtained when the product recovery and oil conversion processes are integrated. This significantly reduces the overall energy input, especially thermal energy, compared to previous predictions in the literature (compare, e.g., 5723 MJ/tonne of camelina oil for our optimized process with heat integration, to 17,628 MJ/tonne of camelina oil predicted by Han et al. [13]). The use of oilseed feedstocks result in higher electricity demand compared to UCO. The electricity demand for oilseed feedstocks in Pearlson [14] and Han et al. [13] is also noticeably lower, perhaps due to different assumptions regarding (or exclusion of) the oil extraction process, which is energy intensive.

The HDO reactions are highly complex and difficult to model, leading to uncertainty in predictions of process yields. Previous studies have constructed simplified HDO process models that relied on UOP's proprietary process data, sufficient for the purpose of estimating process utilities, and relied on generic literature data for H_2 requirements and the product slate. The analysis in this study was based on the selectivity of the deoxygenation reactions and the location of the double bond within each fatty acid chain. This allows prediction of product slates, H_2 demands and utility demands that are specific to each of the camelina, carinata and UCO feedstocks.

There are limited literature data available on process utilities and product yields for the HDO conversion process. Currently, the majority of the publications on HDO conversion are based on a single model developed by Pearlson [14], where process utility estimates have been based on similar unit operations in conventional petroleum processing. While Pearlson [14] has provided a benchmark, the estimated process energy does not include oilseed feedstock handling and processing, which has been found to contribute significantly to the overall process energy demand. Moreover, the reported product yields have been determined from diesel production from soybean oil, and jet fuel production has been inferred from data using jatropha oil. These values have since been cited and widely used to estimate biojet production from various feedstocks, without including the effects of reaction conditions, feedstock compositional differences such as chain lengths, and degree of bond unsaturation, which collectively impact process hydrogen requirements and product yields. When these values are used generically without considering differences due to crop and process yields, process conditions and hydrogen requirements, the evaluation of the associated GHG emissions could be affected, especially for land use change (LUC), which is strongly

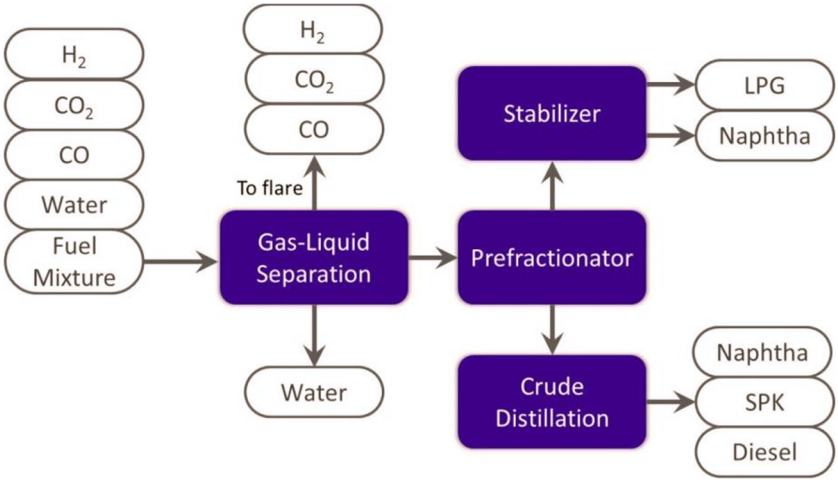

Fig. 5. Block flow diagram of the product purification process.

Table 6
Mass balances for HDO conversion of camelina, carinata and UCO to produce HRJ. Results from Pearlson [14] and Han et al. [13] are presented for comparison.

	Camelina	Carinata	UCO	Pearlson Soyoil	Han et al. Soybean	Han et al. Palm	Han et al. Rapeseed	Han et al. Jatropha	Han et al. Camelina
Input									
Oil	1000	1000	1000	1000	1000	1000	1000	1000	1000
H_2 gas	30	26	26	40	27	22	27	25	30
Output									
CO_2	101	95	104	54	N/R	N/R	N/R	N/R	N/R
CO	2.7	2.5	2.7	N/R	N/R	N/R	N/R	N/R	N/R
Water	36	34	37	87	N/R	N/R	N/R	N/R	N/R
LPG or propane mix	88	79	69	102	78	70	62	78	77
Naphtha	127	145	147	70	57	63	72	57	57
Kerosene	535	537	529	494	740	740	760	740	750
Diesel	140	132	138	233	N/R	N/R	N/R	N/R	N/R

Values expressed per tonne of oil, and mass reported in kg.
N/R – not reported.

Table 7
Thermal energy and electricity requirements for kerosene production via the HDO process using camelina, carinata and UCO. Results from Pearlson [14] and Han et al. [13] are presented for comparison.

Total process energy	Thermal energy, MJ/tonne oil	Electricity, kWh/tonne oil
Camelina	5723	227
Carinata	5185	180
UCO	2820	73
Pearlson, Soyoil	12,473	66
Han et al., Soybean	17,628	45
Han et al., Palm	7013	45
Han et al., Rapeseed	11,036	44
Han et al., Jatropha	11,084	44
Han et al., Camelina	10,809	46

dependent upon crop yields. Han et al. [13] acknowledged the limitations in the HDO process when variations in oil composition are overlooked, and examined the effects of composition on hydrogen requirements for soybean, palm, rapeseed, jatropha and camelina. In Han's study, an increase in hydrogen consumption was observed with an increasing quantity of unsaturated bonds, as expected.

Collectively, our predictions of thermal energy demand are substantially lower than prior literature estimates based upon soy oil, palm oil, jatropha and camelina, illustrating the benefits of comprehensive heat integration among the oil extraction, oil conversion and distillation operations. Compared to the literature, we predict higher electricity demand for processing camelina and carinata, due to the additional energy required for oil extraction, whereas our estimate of electricity demand for UCO is in line with that of the literature. The different thermal and electrical energy requirements predicted by our study would affect the GHG intensity of the HDO process to produce renewable jet fuel.

4. Conclusions

In this study, the effects of feedstock compositional variations on product yields and process utilities were examined, using a model to calculate cracking reactions and the alkane product distribution based upon the fatty acid profile of each feedstock. The yield of kerosene-range alkanes ranged from 53 to 54 wt% of the incoming oil, with 13–14% diesel range alkanes, 13–15% naphtha, and 7–9% LPG, with the balance comprised of water, CO_2, and CO. Feedstocks with a higher degree of bond unsaturation generally consume more hydrogen compared to feedstocks with less unsaturated bonds, although the degree of cracking is also a factor; the consumption rate ranged from 26 to 30 kg per tonne of incoming oil.

Thermal energy demand is 2.8 GJ/tonne oil when processing used cooking oil, versus 5.2 and 5.7 GJ/tonne of oil for carinata and camelina, respectively, owing to the additional energy required for oil extraction. Electricity demand was 73 kWh/tonne oil for UCO, versus 180 and 227 kWh/tonne oil for carinata and camelina. The lower oil content of camelina compared to carinata contributes to the higher thermal and electrical energy demand for the oil extraction process, when expressed per tonne of oil product.

Declaration of interest

The authors have no financial interest in the outcome of this research.

Acknowledgements

This research was financially supported by the Centre for Research in Sustainable Aviation, the Natural Sciences and Engineering Research Council, and the BioFuelNet Network Centre of Excellence.

References

[1] IATA - Halving emissions by 2050 - aviation brings its targets to Copenhagen; 2009. <http://www.iata.org/pressroom/pr/Pages/2009-12-08-01.aspx> [accessed July 20, 2016].
[2] van Renssen S. Climate battle for the skies. Nat Clim Chang 2012;2:308–9. http://dx.doi.org/10.1038/nclimate1493.
[3] Resolution on the implementation of the aviation "CNG2020" strategy 2010. <http://www.iata.org/pressroom/pr/Documents/agm69-resolution-cng2020.pdf> [accessed February 17, 2016].
[4] The EU emissions trading system (EU ETS) 2013. <http://ec.europa.eu/clima/policies/ets/index_en.htm> [accessed July 20, 2016].
[5] EU action-reducing emissions from aviation n.d. <http://ec.europa.eu/clima/policies/transport/aviation/index_en.htm> [accessed July 20, 2016].
[6] Veriansyah B, Han JY, Kim SK, Hong SA, Kim YJ, Lim JS, et al. Production of renewable diesel by hydroprocessing of soybean oil: effect of catalysts. Fuel 2012;94:578–85. http://dx.doi.org/10.1016/j.fuel.2011.10.057.
[7] McCall MJ, Kocal JA, Bhattacharyya A, Kalnes TN, Brandvold TA. Production of aviation fuel from renewable feedstocks. PAT – US 8039682 B2; 2011.
[8] UOP Green Jet Fuel™ Process n.d. <http://www.uop.com/green-jet-fuel/> [accessed July 20, 2016].
[9] Stratton SW. Life cycle assessment of greenhouse gas emissions and non-CO_2 combustion effects from alternative jet fuels. Massachusetts Institute of Technology; 2010.
[10] Shonnard DR, Williams L, Kalnes TN. Camelina-derived jet fuel and diesel: sustainable advanced biofuels. Environ Prog Sustain Energy 2010;29:382–92. http://dx.doi.org/10.1002/ep.10461.
[11] Agusdinata DB, Zhao F, Ileleji K, Delaurentis D. Life cycle assessment of potential biojet fuel production in the United States. Environ Sci Technol 2011;45:9133–43. http://dx.doi.org/10.1021/es202148g.
[12] Fan J, Shonnard DR, Kalnes TN, Johnsen PB, Rao S. A life cycle assessment of pennycress (Thlaspi arvense L.)-derived jet fuel and diesel. Biomass Bioenergy 2013;55:87–100. http://dx.doi.org/10.1016/j.biombioe.2012.12.040.

[13] Han J, Elgowainy A, Cai H, Wang MQ. Life-cycle analysis of bio-based aviation fuels. Bioresour Technol 2013;150:447–56. http://dx.doi.org/10.1016/j.biortech.2013.07.153.
[14] Pearlson MN. A techno-economic and environmental assessment of hydroprocessed renewable distillate fuels. Massachusetts Institute of Technology; 2011.
[15] Pearlson M, Wollersheim C, Hileman J. A techno-economic review of hydroprocessed renewable esters and fatty acids for jet fuel production. Biofuels, Bioprod Biorefining 2013;7:89–96. http://dx.doi.org/10.1002/bbb.1378.
[16] Aspen Technology Inc., Aspen Plus simulation software n.d.
[17] Marillia EF, Francis T, Falk KC, Smith M, Taylor DC. Palliser's promise: Brassica carinata, An emerging western Canadian crop for delivery of new bio-industrial oil feedstocks. Biocatal Agric Biotechnol 2014;3:65–74. http://dx.doi.org/10.1016/j.bcab.2013.09.012.
[18] Gesch RW, Archer DW. Double-cropping with winter camelina in the northern Corn Belt to produce fuel and food. Ind Crops Prod 2013;44:718–25. http://dx.doi.org/10.1016/j.indcrop.2012.05.023.
[19] Cardone M, Mazzoncini M, Menini S, Rocco V, Senatore A, Seggiani M, et al. Brassica carinata as an alternative oil crop for the production of biodiesel in Italy: agronomic evaluation, fuel production by transesterification and characterization. Biomass Bioenergy 2003;25:623–36. http://dx.doi.org/10.1016/S0961-9534(03)00058-8.
[20] Anderson GE. Solvent extraction. Am Oil Chem 2011. <http://lipidlibrary.aocs.org/OilsFats/content.cfm?ItemNumber=40337> [accessed July 20, 2016].
[21] (S&T)2 Consultants INC. Lifecycle analysis canola biodiesel; 2010.
[22] Rispoli K. Life cycle and supply assessment of aviation biofuels from oil feedstock, in the Canadian context. University of Toronto; 2014.
[23] Cheng J, Li T, Huang R, Zhou J, Cen K. Optimizing catalysis conditions to decrease aromatic hydrocarbons and increase alkanes for improving jet biofuel quality. Bioresour Technol 2014;158:378–82. http://dx.doi.org/10.1016/j.biortech.2014.02.112.
[24] Bezergianni S, Voutetakis S, Kalogianni A. Catalytic hydrocracking of fresh and used cooking oil. Ind Eng Chem Res 2009;48:8402–6. http://dx.doi.org/10.1021/ie900445m.
[25] Kim SK, Brand S, Lee HS, Kim Y, Kim J. Production of renewable diesel by hydrotreatment of soybean oil: effect of reaction parameters. Chem Eng J 2013;228:114–23. http://dx.doi.org/10.1016/j.cej.2013.04.095.
[26] Snåre M, Kubičková I, Mäki-Arvela P, Eränen K, Murzin DY. Heterogeneous catalytic deoxygenation of stearic acid for production of biodiesel. Ind Eng Chem Res 2006;45:5708–15. http://dx.doi.org/10.1021/ie060334i.
[27] Moser BR, Vaughn SF. Evaluation of alkyl esters from Camelina sativa oil as biodiesel and as blend components in ultra low-sulfur diesel fuel. Bioresour Technol 2010;101:646–53. http://dx.doi.org/10.1016/j.biortech.2009.08.054.
[28] Dorado MP, Ballesteros E, López FJ, Mittelbach M. Optimization of alkali-catalyzed transesterification of brassica carinate oil for biodiesel production. Energy Fuels 2004;18:77–83.
[29] Haigh KF, Vladisavljević GT, Reynolds JC, Nagy Z, Saha B. Kinetics of the pre-treatment of used cooking oil using Novozyme 435 for biodiesel production. Chem Eng Res Des 2014;92:713–9.